

# Analysis of the Mechanism of Action of Naringin on Nerve-Damaged Cells Based on Nrf2/HO-1 and NF- $\kappa$ B Signaling Pathways

Jian Cui\*, Ni Ye, Daping Wen, Chao Lei, Jun Hang, Gang Wang

Department of Neurosurgery, Xi'an No.1 Hospital, Xi'an 710002, Shaanxi Province, China

\*Corresponding author: Jian Cui, Cuijian16@126.com

**Copyright:** © 2024 Author(s). This is an open-access article distributed under the terms of the Creative Commons Attribution License (CC BY 4.0), permitting distribution and reproduction in any medium, provided the original work is cited.

**Abstract:** *Objective:* To explore the mechanism of action of naringin in protecting nerve-damaged cells through Nrf2/HO-1 and NF- $\kappa$ B signaling pathways. *Methods:* In this study, primary microglia were obtained from 8 neonatal suckling mice and treated with different concentrations of naringin, including a control group (control group) and 4 experimental groups. The activity of primary microglia was assessed using the MTT assay, while apoptosis was evaluated using the TUNEL assay. Molecular biology techniques and cell biology methods were employed to study two types of neuronal cells: highly differentiated PC12 cells and primary microglia. Oxidative stress indicators such as reactive oxygen species (ROS), malondialdehyde (MDA), mitochondrial membrane potential (MMP), and glutathione peroxidase (GSH), as well as inflammatory factors including interleukin-6 (IL-6), interleukin-1 $\beta$  (IL-1 $\beta$ ), and tumor necrosis factor- $\alpha$  (TNF- $\alpha$ ), were detected. Additionally, the expression of related proteins and genes in the Nrf2 signaling pathway and the NF- $\kappa$ B signaling pathway was examined to elucidate the protective effect of naringin on neuronal cells during oxidative stress and inflammation, as well as the underlying mechanism. *Results:* In comparison to the control group, naringin treatment resulted in a statistically significant upregulation of the gene expression of Nrf2 and HO-1 in PC12 cells ( $P < 0.05$ ). Furthermore, compared to the blank control/negative control/model group, naringin notably mitigated the levels of superoxide dismutase, glutathione, malondialdehyde, and nitric oxide in the rats, along with a significant reduction in apoptosis of neurological injury cells ( $P < 0.05$ ). *Conclusion:* Naringin boosts cellular antioxidant capacity by activating the Nrf2/HO-1 signaling pathway, thus mitigating damage to nerve cells inflicted by oxidative stress. Additionally, it reduces the release of inflammatory factors by inhibiting the NF- $\kappa$ B signaling pathway, thereby decreasing inflammation levels. This dual action helps safeguard neural tissues from oxidative and inflammatory damage, ensuring the maintenance of normal nerve cell function.

**Keywords:** Signaling pathway; Naringin; Nerve injured cells; Mechanism of action

**Online publication:** July 22, 2024

## 1. Introduction

Neurodegenerative diseases, commonly afflicting the elderly, are characterized by the loss or atrophy of central nervous system neurons or their myelin sheaths, resulting in neurological dysfunction. Conditions like

Parkinson's (PD) and Alzheimer's (AD) are prominent examples, featuring neuronal loss and behavioral and memory dysfunctions<sup>[1-2]</sup>. Despite ongoing research into their pathogenesis, treatments for neurodegenerative diseases remain underdeveloped. Evidence suggests a correlation between these diseases and oxidative stress and inflammation<sup>[3-4]</sup>. Oxidative processes are ubiquitous in the animal body, yet they do not typically result in pathological changes thanks to the presence of an inherent antioxidant mechanism. This mechanism effectively counterbalances oxidation, maintaining equilibrium within the body. However, oxidative stress arises when oxidized products accumulate due to inadequate removal, leading to bodily damage<sup>[5]</sup>. Numerous diseases, including cerebral ischemia and diabetes, have been directly linked to oxidative stress. For instance, oxidative stress plays a role in the early response to cerebral ischemia, potentially contributing to ischemic brain injury<sup>[6-7]</sup>. Additionally, insulin resistance, a key factor in diabetes development, may also be influenced by oxidative stress and inflammation. In many disease contexts, inflammation and oxidative stress often occur concurrently, suggesting a close interconnection between the two processes<sup>[8-9]</sup>. Research has shown that cardiovascular diseases like arrhythmias, Parkinson's, Alzheimer's disease, and coronary heart disease are linked to inflammation and oxidative stress<sup>[10]</sup>. Since inflammation and oxidative stress are often associated with neurodegenerative diseases, it has been demonstrated that oxidative stress and inflammation are one of the causes of neurodegenerative diseases and that these two processes are interrelated and mutually reinforcing<sup>[11]</sup>. Reactive oxygen species (ROS) generated by oxidative stress can trigger inflammation, and the inflammatory response, in turn, works to dampen ongoing inflammation. Building upon this understanding, this study was carried out to delve deeper into the protective mechanism of naringin against nerve injury using cellular and molecular biology techniques. By leveraging previous research, we aim to offer novel insights and a scientific basis for the potential therapeutic application of naringin in treating these diseases in clinical settings.

## 2. Materials and instruments

### 2.1. Experimental materials and reagents

(1) Eight neonatal suckling mice (1–2 days old) obtained from Beijing Spivet Biotechnology Co., Ltd, with Animal Qualification Certificate No. SCXK (Beijing) 2019-0010; (2) 75% alcohol; (3) D-hanks buffer, 0.125% trypsin (containing EDTA and DNase enzyme), and DMEM/F12 complete culture medium containing FBS acquired from Thermo Fisher Scientific; (4) naringin; (5) 0.01 M PBS, 4% PFA (paraformaldehyde), Proteinase K dilution, TdT (nucleic acid transferase), DIG-dUTP, biotin-labeled anti-digoxin antibody, and SABC diluent procured from Isejyu Technology Co., Ltd.; (6) DAPI (4',6-diamidino-2-phenylpyridine) and an inflammatory factor detection kit (for detecting TNF- $\alpha$ , IL-6, IL-1 $\beta$ ) purchased from Saikoku Technology Co.

### 2.2. Experimental instruments

**Table 1.** Main instruments

Instrument name	Model	Manufacturer
Centrifuge	Eppendorf 5424R	Fisher Scientific
Cell counter plate	Neubauer Improved	Thermo Fisher Scientific
5% CO <sub>2</sub> Incubator	Thermo Scientific CO <sub>2</sub> Incubator	Thermo Fisher Scientific
Needle filter (0.22 $\mu$ m)	Millipore Stericup	Millipore Sigma
Microscopy	Nikon Eclipse	Nikon
Fluorescence microscope	Olympus IX83	Olympus

### **3. Methods**

#### **3.1. Primary microglia culture**

##### **3.1.1. Mixed glial cell culture**

(1) Eight neonatal suckling mice aged 1–2 days were selected and sterilized by soaking them in 75% alcohol for 1–2 minutes. (2) Under aseptic conditions, the suckling mice were decapitated, and a craniotomy was performed to remove the brain. The brain was then rinsed 2–3 times with pre-cooled D-hanks buffer to remove blood. (3) The meninges, blood vessels, and brain stem were carefully removed, and the cerebral hemispheres were extracted and cut into approximately  $0.5 \times 0.5 \times 0.5$  mm pieces using ophthalmic scissors. (4) The tissue was centrifuged at 1000 rpm for 5 minutes, and the supernatant was discarded. Approximately 2–3 times the volume of 0.125% trypsin (containing EDTA and DNase enzyme) was added, and the tissue was gently digested for 40–60 minutes in a 37 °C water bath. The tissue was blown with a pipette 2–3 times halfway through the process until no obvious tissue clumps were observed. (5) DMEM/F12 complete medium containing FBS was added to terminate the digestion, and the mixture was resuspended by repeated blowing. The suspension was passed through a 200-mesh cell sieve and centrifuged at 1000 rpm for 5 minutes. (6) The supernatant was discarded, and the cells were resuspended. The cell density was adjusted to  $1 \times 10^6$  cells/mL, and the cells were inoculated into 50 mL culture flasks pre-coated with Poly-L-lysine (PLL). The flasks were placed at 37°C in a 5% CO<sub>2</sub> incubator. (7) The complete medium was replaced after 4 hours, and thereafter, half of the medium was replaced every 3 days until the mixed glial cell stratification appeared after 7–9 days.

##### **3.1.2. Microglia isolation and purification**

(1) A half-volume change of the medium was performed the day before cell stratification. (2) After cell stratification, the culture bottle was sealed with sealing film. The bottle mouth was held upward with the right hand, and the bottom surface of the bottle was gently tapped with the palm of the left hand at a 45-degree angle while observing the cell detachment under the microscope. (3) The cell supernatant was collected into a new culture flask (PLL-coated) and left in the incubator for 15–30 minutes. (4) Afterward, the complete medium was replaced, and half the amount of fresh medium was added. The original medium was filtered through a 0.22 µm needle filter before being added to the culture flask. (5) The microglia adhering to the wall were observed, and they were incubated for 1–2 days after isolation for experiments.

#### **3.2. Protective effect of naringin on microglia**

##### **3.2.1. Naringin concentration screening and MTT assay for cell activity**

(1) Naringin of 5 concentrations were prepared (0 µm, 1 µm, 10 µm, 100 µm, and 1,000 µm), which would act as the controls in this experiment. (2) Microglial cells at a concentration of 2.0 µg/L were selected as the experimental model. (3) Six concentration gradients were set in the range of 10–160 µM/L: 0 µM, 10 µM, 20 µM, 40 µM, 80 µM, and 160 µM. (4) The activity of microglia was determined using the MTT assay, which utilizes the succinate dehydrogenase enzyme in the living cells to reduce exogenous MTT to a water-insoluble purple precipitate. (5) After treatment with the MTT method, a blue-violet purple precipitate was observed in the cells. (6) The purple precipitate could be dissolved by adding DMSO to the cells.

##### **3.2.2. Detection of apoptosis of primary cultured microglia by the TUNEL method**

(1) The digested primary cells were resuspended, and the cell density was adjusted to  $1 \times 10^5$  cells/ml. Then, 0.5 mL of cell suspension was inoculated per well into a 24-well plate with PLL coating. (2) After culturing the cells for 1-2 days, the medium containing the drug was replaced to treat the cells for 24 hours. At the end of the treatment, the original medium was aspirated. (3) The slides were washed with 0.01M PBS for 2 minutes each

time and 3 times in total. Then, the cells were fixed with 4% PFA for 30 minutes and digested with Proteinase K dilution for 30 seconds (dilution ratio: 1:200 using 0.01M TBS). Afterward, the slides were washed with 0.01M TBS for 2 minutes each time and 3 times in total. (4) The labeling solution was prepared by adding 1  $\mu$ L TdT, 1  $\mu$ L DIG-dUTP, and 18  $\mu$ L labeling buffer per slide. The slides were placed in a wet box and incubated at 37°C for 2 hours. (5) The slides were washed using 0.01 M TBS for 2 minutes each time for a total of 3 washes, followed by a 30-minute sealing treatment without washing. (6) Biotin-labeled anti-digoxin antibody (1:100) was added dropwise at 50  $\mu$ L per slide in a wet box and incubated at 37°C for 30 minutes. Then, the slides were washed using 0.01 M TBS for 2 minutes each time for a total of 3 washes. (7) SABC dilution (1:100) was added dropwise at 50  $\mu$ L per slice, and the slides were reacted at 37°C for 30 minutes. After that, the slides were washed using 0.01 M TBS for 5 minutes each time, and a total of 4 times. Subsequently, DAPI light staining was carried out, and the slides were sealed after washing. (8) The results were observed using a fluorescence microscope, and photographs were taken. Yellow-green particles in the nucleus were observed as a positive signal to determine whether apoptosis occurred in the cells.

### **3.2.3. Detection of inflammatory factor content in microglia**

(1) Glial cells in the logarithmic growth phase were harvested and subjected to digestion using 0.25% trypsin. After that, the cells were gently dispersed by blowing them in a medium containing 10% FBS to ensure uniform distribution. (2) The cells were counted, and the density was adjusted to  $1 \times 10^7$  cells/mL. Then, they were inoculated into a 6-well cell culture plate for backup. (3) Once the cells covered the entire bottom of the wells, the medium was replaced with fresh medium, and treatment was initiated. (4) After treatment, cells were collected by scraping and transferred to 1.5 mL centrifuge tubes. The tubes were centrifuged at 1000 rpm for 5 minutes, and the supernatant was collected for the detection of inflammatory factors TNF- $\alpha$ , IL-6, and IL-1 $\beta$ .

## **3.3. Effects of naringin on oxidative stress in PC12 cells**

### **3.3.1. Determination of ROS content**

(1) PC12 cells were treated using the in situ probe loading method, and then the cells were collected. (2) The content of ROS in the cells was determined using flow cytometry.

### **3.3.2. Measurement of malondialdehyde content**

(1) PC12 cells were washed with pre-cooled PBS solution and then collected in a centrifuge tube. (2) The cells were treated with lysate, and the supernatant was collected as the sample. (3) The malondialdehyde content in the sample was determined using a malondialdehyde kit.

### **3.3.3. Determination of glutathione peroxidase content**

(1) Samples were prepared using a sample preparation method similar to that used for determining malondialdehyde content. (2) NADPH solution, GSH solution, GPx assay working solution, and peroxide reagent solution were prepared. (3) The blank control, sample background control, and sample group were set up. Different reagents were added into a 96-well plate and mixed well, and the absorbance value at 340 nm was measured using an enzyme marker.

### **3.3.4. Mitochondrial membrane potential assay**

(1) PC12 cells were treated with JC-1 staining working solution, followed by collection, centrifugation, and removal of the supernatant. (2) The cells were washed with JC-1 staining buffer, and finally, they were detected by flow cytometry.

### 3.4. Study on the mechanism of action of naringin

After isolating primary microglia and culturing PC12 cells as described above, the cells were subjected to intervention using NF- $\kappa$ B-specific antibody and Nrf2-specific antibody. Subsequently, the Western blot method and RT-PCR were employed for further testing.

#### 3.4.1. RT-PCR method

(1) Total RNA was extracted from the cells using TRIzol reagent (Invitrogen, USA). (2) Reverse transcription of 1  $\mu$ g RNA was conducted to synthesize cDNA. (3) PCR reactions were carried out on a BioRad CFX96 real-time quantitative PCR platform using primers and probes specific to the target genes. The GAPDH gene was chosen as the internal reference gene. (4) The mRNA expression levels of the target gene (e.g., NPRA) were compared using the  $\Delta\Delta$ CT method.

#### 3.4.2. Western blot assay

(1) Cultured neural cells were transferred into pre-cooled lysis solution (containing Tris-HCL 20, NaCl 50, NaF 50,  $\text{Na}_4\text{P}_2\text{O}_7$  50, Sucrose 250,  $\text{Na}_3\text{VO}_4$  2, DTT 1 mmol/L and 1 % complex protease inhibitor) and lysed. (2) The protein content in the lysate was quantified using the BCA protein quantification kit. (3) The protein samples were separated by SDS-PAGE electrophoresis and transferred onto a PVDF membrane (Bio-Rad, USA). (4) The PVDF membrane was blocked with 5% skimmed milk powder for 1 h at room temperature. (5) After blocking, the membrane was incubated with specific primary antibodies overnight at 4°C. (6) Subsequently, the membrane was washed with PBST buffer and incubated with secondary antibodies for 1 h at 37°C. (7) Following the removal of unbound secondary antibodies, chemiluminescence detection was performed using the ECL-plus immunoassay kit.

### 3.5. Statistical methods

Statistical analysis was performed using the SPSS 26.0 software. Measurements were presented as mean  $\pm$  standard deviation, and a one-way ANOVA was used for multiple group comparisons. Statistical significance was considered at  $P < 0.05$ .

## 4. Results

### 4.1. Hypothesis

We hypothesized that naringin protects against nerve injury by mediating the Nrf1/HO-1 and NF- $\kappa$ B signaling pathways. We established cellular inflammation and oxidative stress nerve injury models by culturing neuronal cells, highly differentiated PC12 cells, and microglial cells in vitro and inducing LPS and  $\text{H}_2\text{O}_2$ . The induction of LPS and  $\text{H}_2\text{O}_2$  creates an oxidative stress neurological injury model, and subsequently, naringin is administered at varying concentrations to address the “inflammatory and oxidative stress-mediated neurological injury disorders” and protect the neural cells. Further details are shown in **Figure 1**.

### 4.2. Protective effect of naringin against $\text{H}_2\text{O}_2$ -induced oxidative stress in PC12 cells and LPS-induced inflammation in primary microglial cells

In the treated PC12 cells, naringin up-regulated the gene expression of Nrf2 and HO-1 compared to the control group. This indicates that at the cellular level, naringin exhibits a protective effect on nerve-injured cells, particularly by suppressing the expression of Nrf2 and HO-1 (**Figure 2**).

### 4.3. Study of naringin's mechanism on nerve injury cell damage

Naringin exhibited a significant ability to attenuate superoxide dismutase, glutathione, malondialdehyde, and nitric oxide levels in rats, along with a notable reduction in apoptosis of nerve-injured cells (Figure 3).

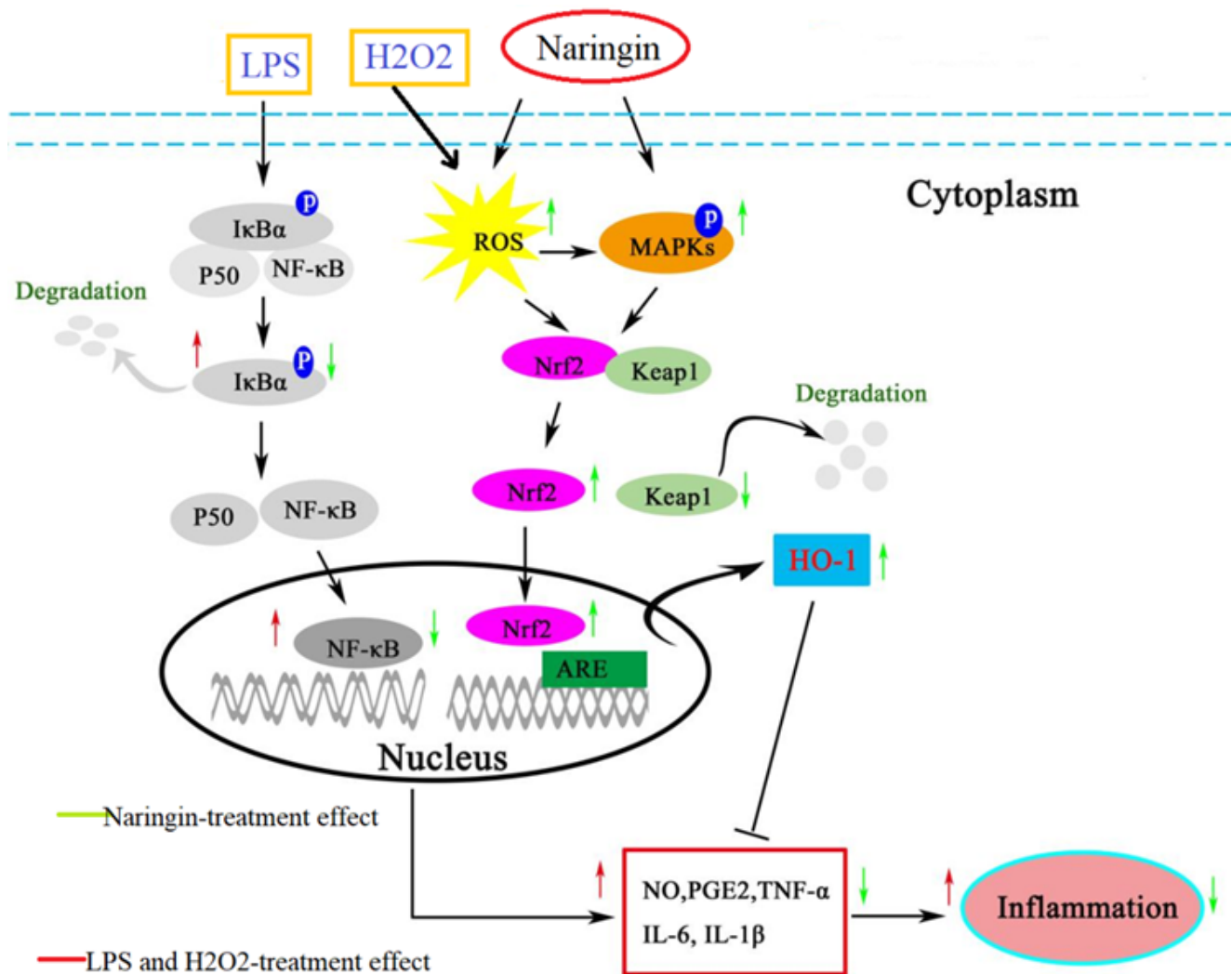


Figure 1. Hypothesis

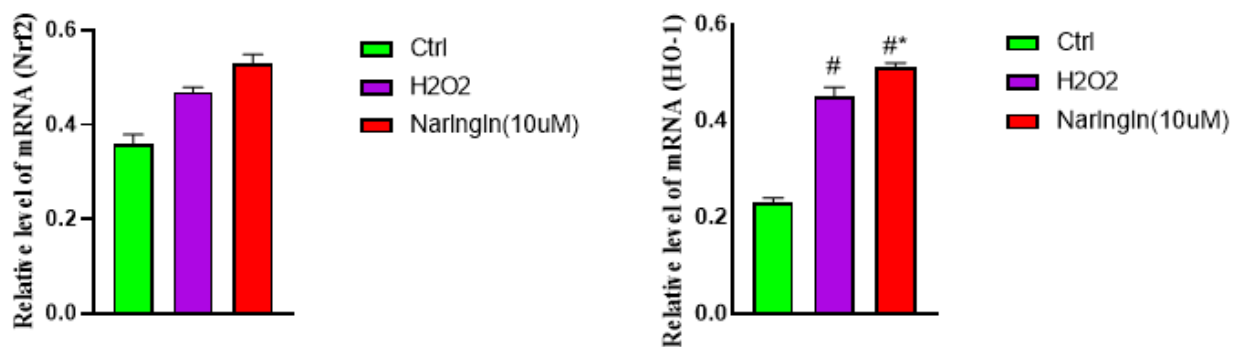
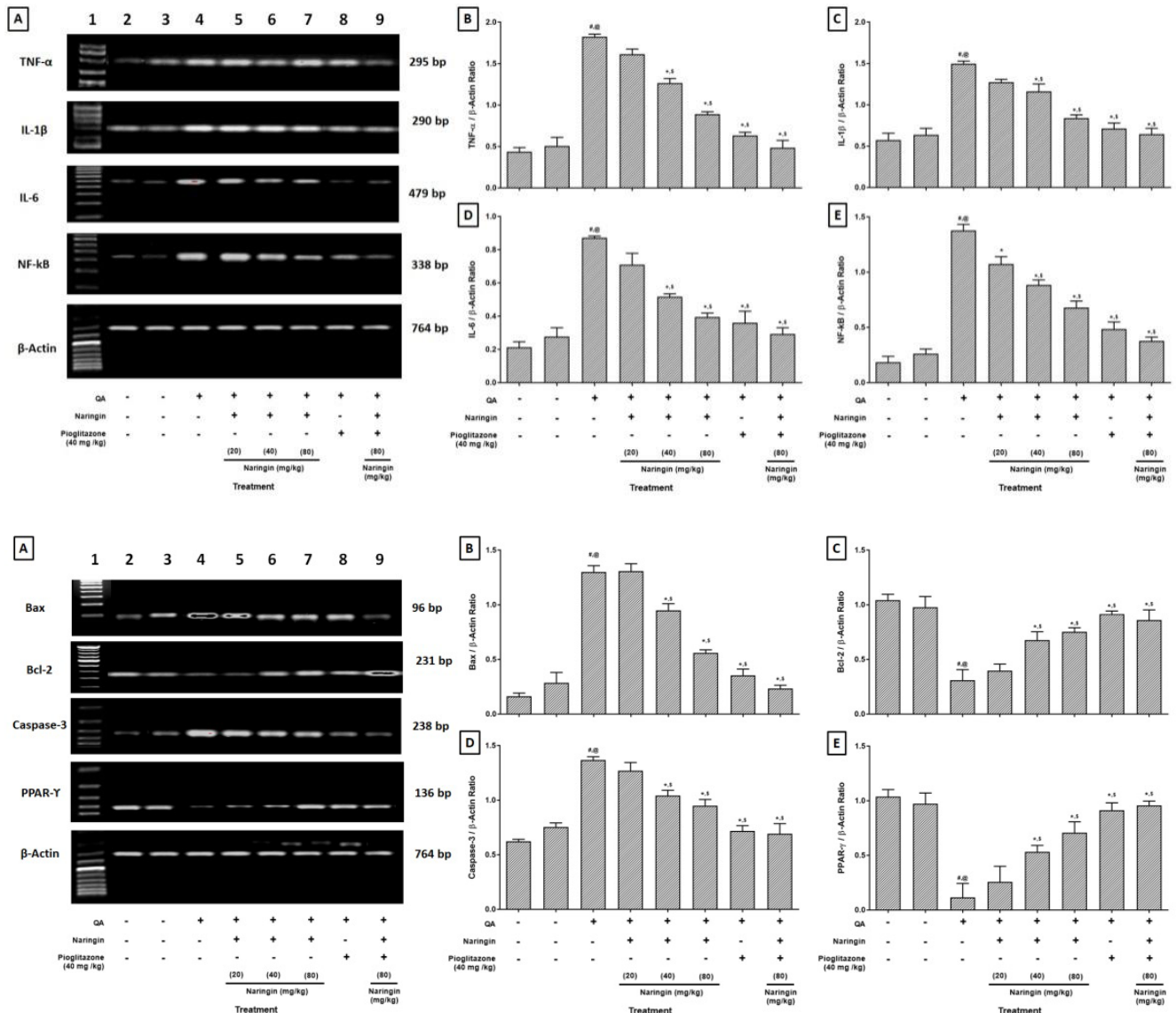


Figure 2. Genetic changes of Nrf2 and HO-1 in PC12 cells induced by H<sub>2</sub>O<sub>2</sub> by naringin. Note: Data expressed as mean ± SEM (n = 4), #P < 0.05 vs blank control group, \*P < 0.05 vs model group.



**Figure 3.** Striatal gene changes in quinolinic acid-induced nerve injury by naringin. Note: Data expressed as Mean ± SEM ( $n = 4$ ), # $P < 0.05$  vs blank control group, @ $P < 0.05$  vs negative control group, \* $P < 0.05$  vs model group.

## 5. Discussion

The research on Chinese medicines and their active ingredients has gained increasing recognition. Chinese medicines are distinguished from Western medicines by their multi-target and multi-pathway actions, along with their reliable and cost-effective active ingredients, making them suitable for broad clinical applications. Various traditional Chinese medicines, such as naringin, rhododendron, and lianchonin, are currently undergoing in-depth studies to elucidate their mechanisms of action [12–14]. Naringin, a natural flavonoid found primarily in the fruits or peels of rutaceous plants like grapefruit and lime, has been subject to extensive research in recent years. Its diverse benefits have been highlighted across various studies. In the context of gestational diabetes, naringin demonstrates the potential to improve body weight and blood glucose levels, as well as reduce insulin resistance in mouse models. Activation of the AMPK-GLUT4 pathway and the promotion of glucose metabolism appear to be key mechanisms underlying its efficacy in reducing insulin resistance [15]. Additionally, naringin has demonstrated the ability to inhibit ventricular remodeling by reducing cardiomyocyte apoptosis

and inflammation [16]. Furthermore, naringin has been implicated in anti-vasodilation and improving learning and memory [17–18]. Its antioxidant and anti-inflammatory properties have also been well documented [19].

A previous pre-course group study [20–21] demonstrated that therapeutic doses of naringin (40 mg/kg and 80 mg/kg) significantly ameliorated quinolinic acid-induced alterations in motor behavior, neural scores, and footprints in rats, as depicted in **Figure 4**, indicating its potential in alleviating behavioral changes in nerve-injured rats. Building upon this, the present study further revealed that naringin upregulated the expression levels of Nrf2 and HO-1 genes in PC12 cells. Moreover, naringin significantly reduced the levels of superoxide dismutase, glutathione, malondialdehyde, and nitric oxide in rats, while notably decreasing the apoptosis rate of nerve-injured cells.

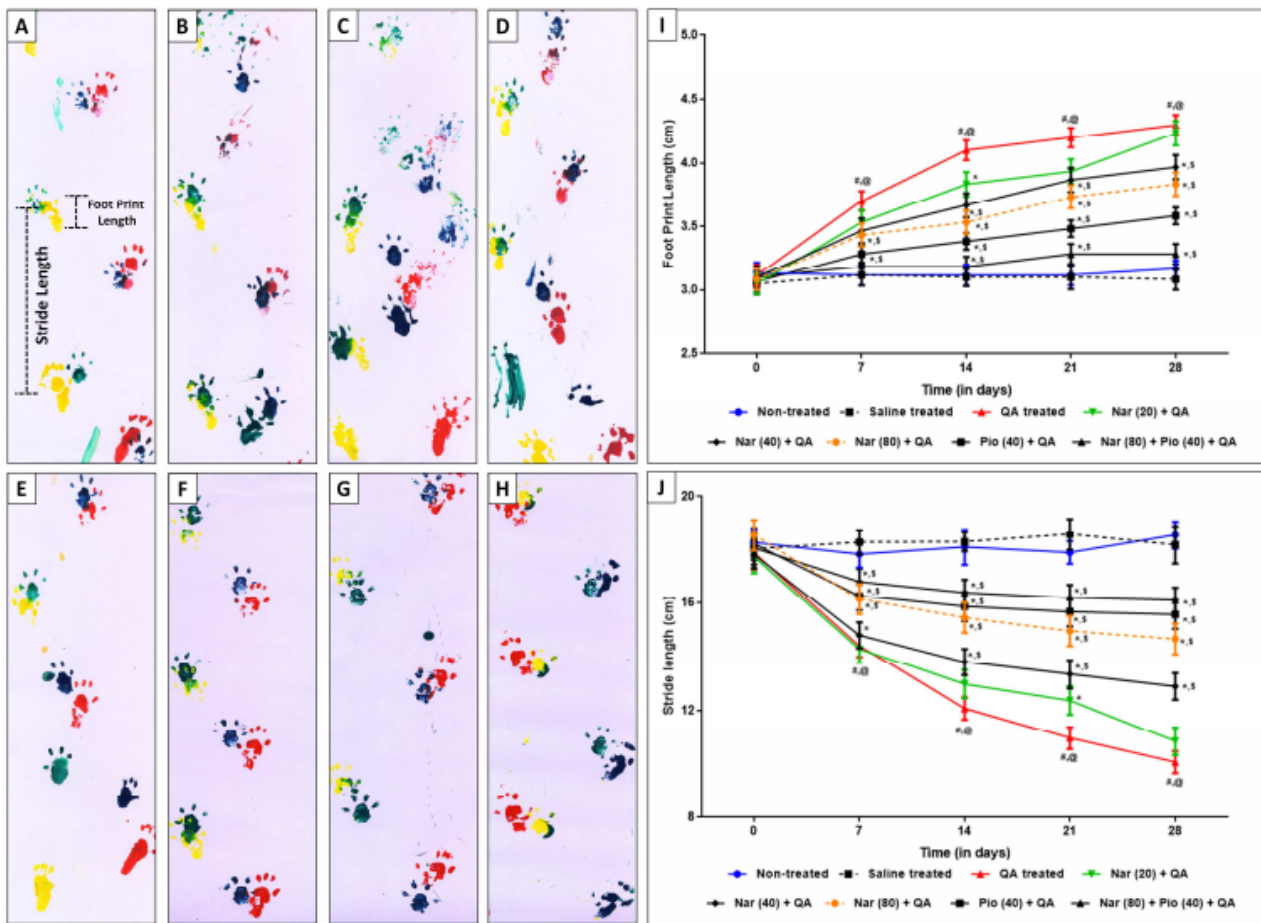


**Figure 4.** Footprint analysis of naringin on quinolinic acid-induced nerve injury in rats

Note: (A) Blank control group, (B) Negative control group, (C) Model group, (D) Naringin 20mg/kg, (E) Naringin 40mg/kg, (F) Naringin 80mg/kg, (G) Pioglitazone 40mg/kg, (H) Pioglitazone 80mg/kg. I and J represent the quantitative analyses of naringin's effect on the change of step width of footprint length in quinlorac-induced nerve injury rats. The data are presented as mean ± SEM (n = 6). #P < 0.05 vs. blank control group, @P < 0.05 vs. negative control group, and \*P < 0.05 vs. model group

## 6. Conclusion

In summary, the mechanism of action of naringin involves two main aspects. Firstly, it activates the Nrf2/HO-1 signaling pathway, thereby enhancing the antioxidant capacity of cells. This leads to an increase in the expression and activity of the antioxidant enzyme HO-1, effectively mitigating the damage caused by oxidative



stress to nerve-damaged cells and offering protection against oxidative damage. Secondly, naringin may suppress the release of inflammatory factors and the onset of inflammatory responses by inhibiting the activity of the NF- $\kappa$ B signaling pathway. This helps to reduce inflammation levels in nerve-damaged cells, alleviate inflammatory damage to nerve tissues, and preserve the normal function of nerve cells. In short, naringin likely regulates the extent of nerve injury through the Nrf2/HO-1 and NF- $\kappa$ B signaling pathways, providing valuable insights for the clinical treatment of nerve injury-related conditions and serving as an experimental foundation for the development of novel therapeutic agents.

## Disclosure statement

The authors declare no conflict of interest.

## References

- [1] Gubert C, Kong G, Renoir T, et al., 2020, Exercise, Diet and Stress as Modulators of Gut Microbiota: Implications for Neurodegenerative Diseases. *Neurobiology of Disease*, 134: 104621.
- [2] Zhang P, Cui J, Mansooridara S, et al., 2020, Suppressor Capacity of Copper Nanoparticles Biosynthesized using *Crocus sativus* L. Leaf Aqueous Extract on Methadone-Induced Cell Death in Adrenal Pheochromocytoma (PC12) Cell Line. *Scientific Reports*, 10(1): 11631.
- [3] Rekatsina M, Paladini A, Piroli A, et al., 2020, Pathophysiology and Therapeutic Perspectives of Oxidative Stress and Neurodegenerative Diseases: A Narrative Review. *Advances in Therapy*, 37(1): 113–139.
- [4] Wang JL, Xu CJ, 2020, Astrocytes Autophagy in Aging and Neurodegenerative Disorders. *Biomedicine & Pharmacotherapy*, 122: 109691.
- [5] Filomeni G, De Zio D, Cecconi F, 2015, Oxidative Stress and Autophagy: The Clash Between Damage and Metabolic Needs. *Cell Death and Differentiation*, 22(3): 377–388.
- [6] Li X, Cheng S, Hu H, et al., 2020, Progranulin Protects Against Cerebral Ischemia-Reperfusion (I/R) Injury by Inhibiting Necroptosis and Oxidative Stress. *Biochemical and Biophysical Research Communications*, 521(3): 569–576.
- [7] Wu L, Xiong X, Wu X, et al., 2020, Targeting Oxidative Stress and Inflammation to Prevent Ischemia-Reperfusion Injury. *Frontiers in Molecular Neuroscience*, 13: 28.
- [8] Ahmad A, Ahsan H, 2020, Biomarkers of Inflammation and Oxidative Stress in Ophthalmic Disorders. *Journal of Immunoassay & Immunochemistry*, 41(3): 257–271.
- [9] Pegoretti V, Swanson KA, Bethea JR, et al., 2020, Inflammation and Oxidative Stress in Multiple Sclerosis: Consequences for Therapy Development. *Oxidative Medicine and Cellular Longevity*, 2020: 7191080.
- [10] McGarry T, Biniiecka M, Veale DJ, et al., 2018, Hypoxia, Oxidative Stress and Inflammation. *Free Radical Biology & Medicine*, 125: 15–24.
- [11] Zuo L, Prather ER, Stetskiv M, et al., 2019, Inflammaging and Oxidative Stress in Human Diseases: From Molecular Mechanisms to Novel Treatments. *International Journal of Molecular Sciences*, 20(18): 4472.
- [12] Yu KE, Alder KD, Morris MT, et al., 2020, Re-Appraising the Potential of Naringin for Natural, Novel Orthopedic Biotherapies. *Therapeutic Advances in Musculoskeletal Disease*, 12: 1759720X20966135.
- [13] Dong X, Fu J, Yin X, et al., 2016, A Review of its Pharmacology, Toxicity and Pharmacokinetics. *Phytotherapy Research*, 30(8): 1207–1218.
- [14] Wang L, Zhang W, Lu Z, et al., 2020, Functional Gene Module-Based Identification of Phillyrin as an Anticardiac Fibrosis Agent. *Frontiers in Pharmacology*, 11: 1077.

- [15] Dai P, Cui C, Liu Y, et al., 2020, Mechanism of Improvement of Insulin Resistance by Naringin in Gestational Diabetic Mice. *Chinese Journal of Clinical Pharmacology*, 36(22): 3747–3750.
- [16] Mo L, Wu K, 2015, GW26-e4796 Effect of Naringin on Myocardial Remodeling by Regulating the Expression of FABP4, FFA in Rats with Diabetes Cardiomyopathy. *Journal of the American College of Cardiology*, 66(16): C130.
- [17] Slámová K, Kapešová J, Valentová K, 2018, “Sweet Flavonoids”: Glycosidase-Catalyzed Modifications. *International Journal of Molecular Science*, 19(7): 2126.
- [18] Kola PK, Akula A, Nissankara RLS, et al., 2017, Protective Effect of Naringin on Pentylentetrazole (PTZ)-Induced Kindling; Possible Mechanisms of Antikindling, Memory Improvement, and Neuroprotection. *Epilepsy & Behavior.*, 75: 114–126.
- [19] Nilamber LDR, Muruhan S, Nagarajan RP, et al., 2019, Naringin Prevents Ultraviolet-B Radiation-Induced Oxidative Damage and Inflammation Through Activation of Peroxisome Proliferator-Activated Receptor  $\Gamma$  in Mouse Embryonic Fibroblast (NIH-3T3) Cells. *Journal of Biochemical and Molecular Toxicology*, 33(3): e22263.
- [20] Cui J, Wang G, Kandhare AD, et al., 2018, Neuroprotective Effect of Naringin, a Flavone Glycoside in Quinolinic Acid-Induced Neurotoxicity: Possible Role of PPAR- $\gamma$ , Bax/Bcl-2, and Caspase-3. *Food and Chemical Toxicology*, 121: 95–108.
- [21] Zhang P, Cui J, Mansooridara S, et al., 2020, Suppressor Capacity of Copper Nanoparticles Biosynthesized Using *Crocus sativus* L. Leaf Aqueous Extract on Methadone-Induced Cell Death in Adrenal Pheochromocytoma (PC12) Cell Line. *Scientific Reports*, 10(1): 11631.

**Publisher's note**

Bio-Byword Scientific Publishing remains neutral with regard to jurisdictional claims in published maps and institutional affiliations.